

CREX

Ryan Richards
University of Virginia

Outline

- Elastic Electron Scattering
- Parity Violating Elastic Electron Scattering
- Motivation
- Experimental Overview
- A_{PV} Measurements
- $R_n - R_p$
- Summary

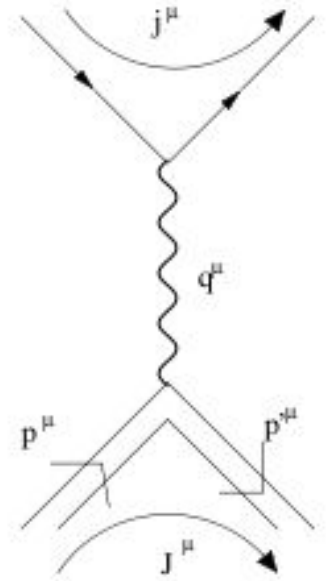
Electromagnetic Elastic Electron Scattering

So what would elastic electron scattering tell us?

$$\frac{d\sigma}{d\Omega} = \frac{d\sigma}{d\Omega} \Big|_{\text{Mott pointlike}} \times |F(Q^2)|^2$$

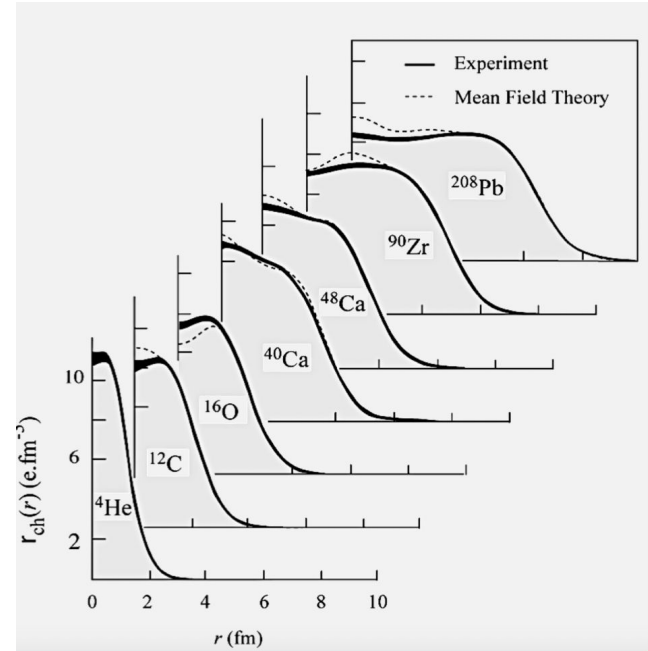
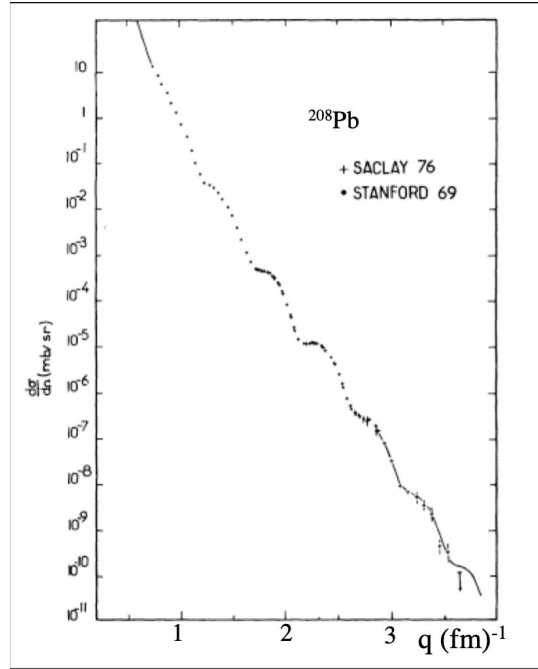
pointlike \times structure

- Cross section factorizes into a point-like part and a structure part.
- Structure part depends on the momentum transfer $Q^2 = 2EE'(1-\cos\theta)$.
- $F(Q^2)$ is the form factor - static properties of the nuclei e.g., charge distribution.
- $F(Q^2)$ is the Fourier transform of the charge distribution.



Elastic Electron Scattering

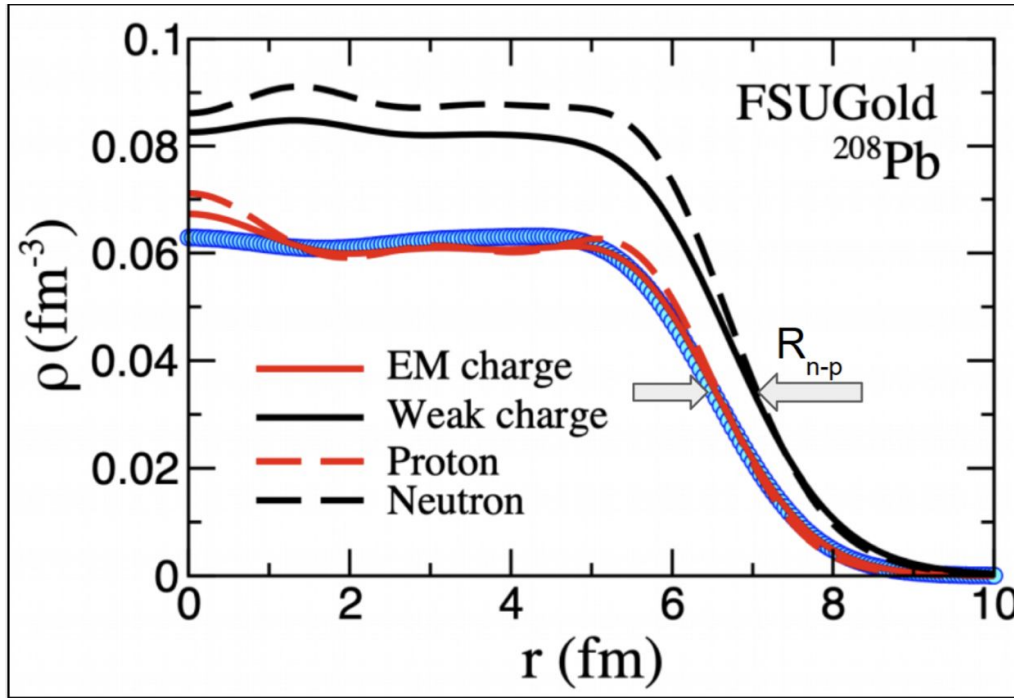
Elastic Electron Scattering off spin-0 through γ Exchange provides R_p through form factors



Small Q^2 for spin 0 nuclei

$$F(Q^2) \approx F(0) + Q^2 \left. \frac{dF}{dQ^2} \right|_{Q^2=0} + \dots = \int \rho(\vec{x}) d^3x - \frac{1}{6} Q^2 \langle r_{\text{charge}}^2 \rangle + \dots$$

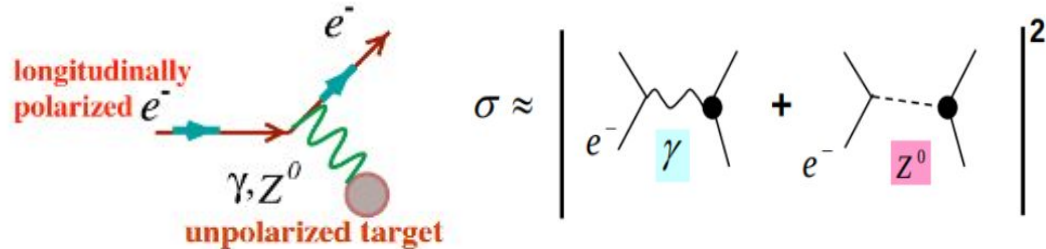
Weak Charge Distribution



^{208}Pb as an example

- Nuclear theory predicts a neutron “skin” for heavy(ish) nuclei.
- However, knowledge of neutron distribution R_n is model dependent and not well constrained by measurements. Neutrons are hard to measure!
- Make use of the fact that the weak charge of the proton (~ 0.08) is much less than the weak charge of the neutron (~ 1)
- So neutron distribution closely matches the weak charge distribution
- Therefore measure F_w

Parity-Violating Electron Scattering

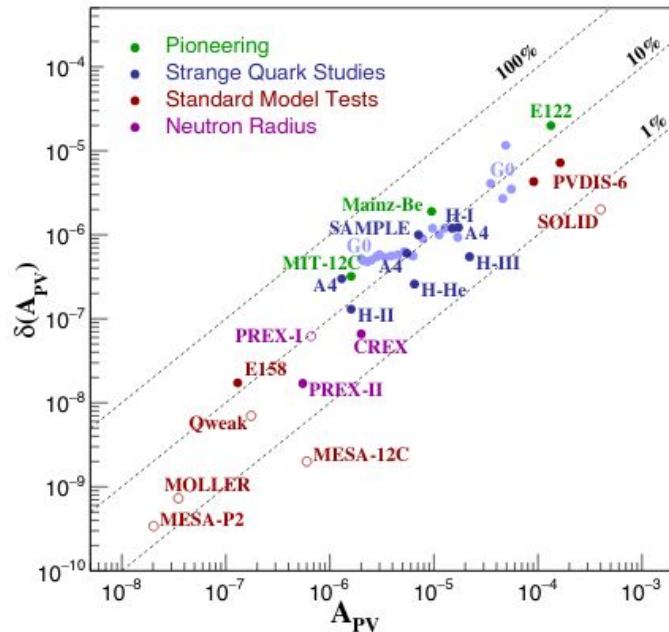


Measure fraction rate difference - parity-violating asymmetry

$$A_{PV} = \frac{\sigma_+ - \sigma_-}{\sigma_+ + \sigma_-} \propto \frac{\left| \begin{array}{c} \gamma \\ \text{---} \\ \end{array} \right| \left| \begin{array}{c} Z^0 \\ \text{---} \\ \end{array} \right|}{\left| \begin{array}{c} \gamma \\ \text{---} \\ \end{array} \right|^2} \propto \frac{|M_Z|}{|M_\gamma|}$$

Electroweak interference

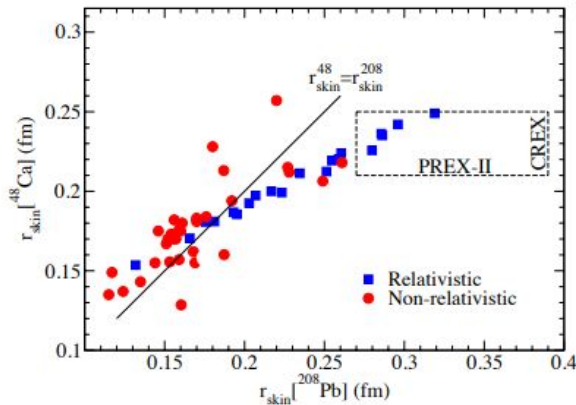
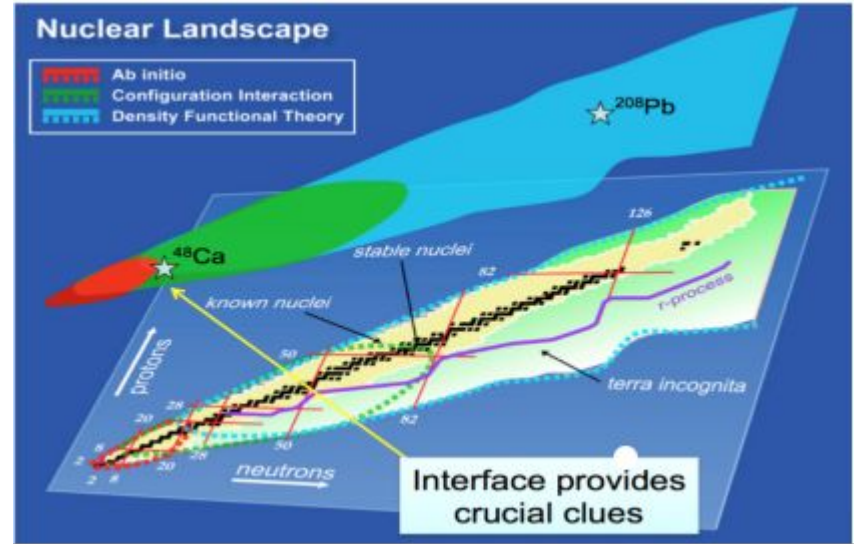
$$A_{PV} \sim \frac{Q^2}{M_Z^2} 10^{-7} - 10^{-4} \quad A_{PV} \approx \frac{Q^2}{4\pi\alpha\sqrt{2}M_Z^2} \frac{F_n(Q^2)}{F_p(Q^2)}$$



PVES has been used as a precision tool to probe nuclear structure, BSM

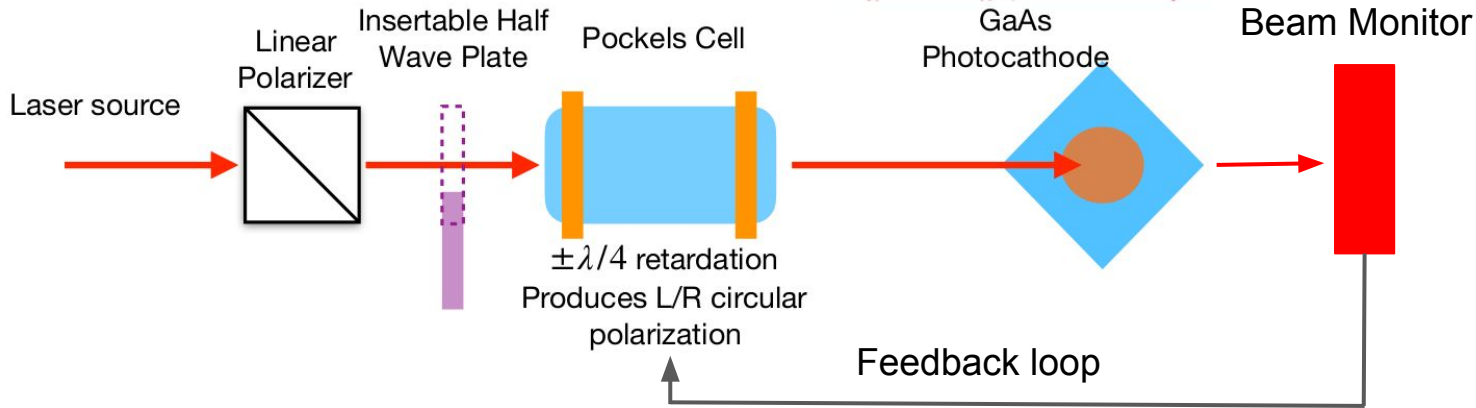
Motivation

- ^{208}Pb can be well described using density functional theory (DFT)
- Although applicable to nuclear landscape, works best with medium to heavy nuclei
- Ab initio (exact microscopic) calculations describe light to medium nuclei using 2 and 3 nucleon forces
- ^{48}Ca would provide a bridge between ab initio approaches and DFT

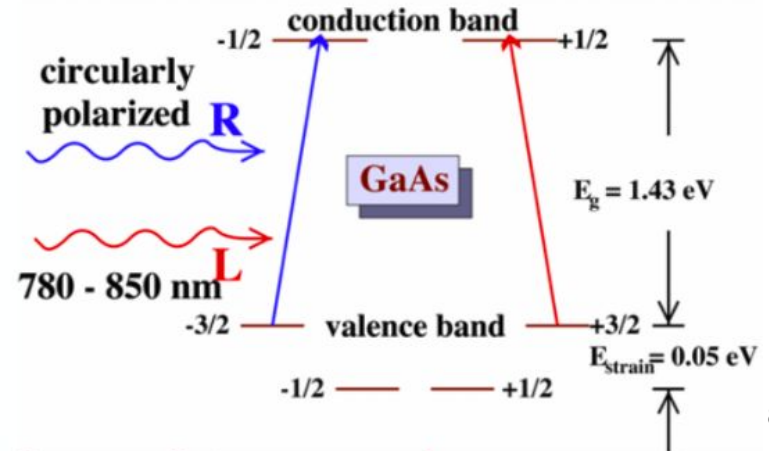


- DFTs show correlation between the neutron skin of ^{208}Pb and ^{48}Ca , however, this depends on how correct the model is.
- Precision measurement of the neutron skin for ^{48}Ca together with the PREX-II measurement would allow us to test models over a wide range of A

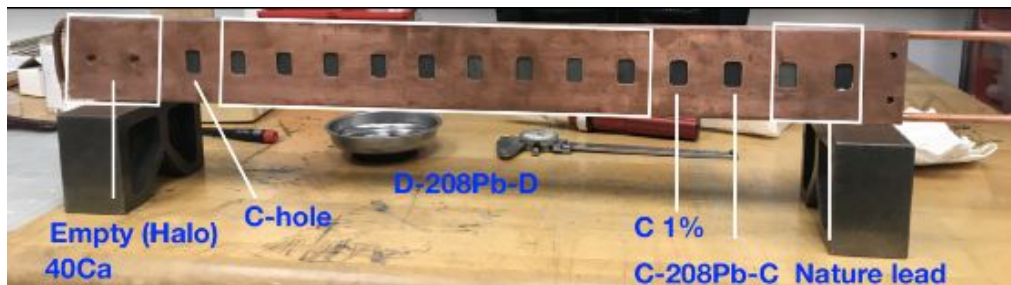
Polarized Source



- L/RCP light produced by Pockels cell
- **Rapid helicity reversal** - Pockels cell
- **Slow helicity reversal** - **Insertable Half Wave Plate** inserted in optical path : changes sign of phase shift induced by Pockels cell. **Double Wien filter**: Manipulates spin - reverse polarization of electron beam relative to the polarization of the laser light

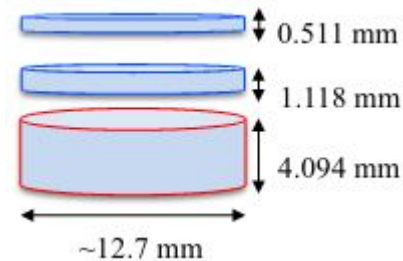
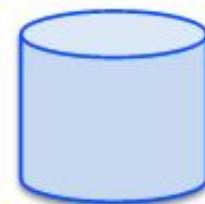
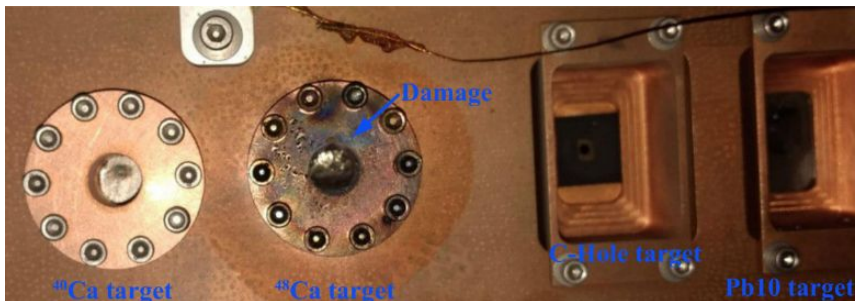


CREX Target and Kinematics

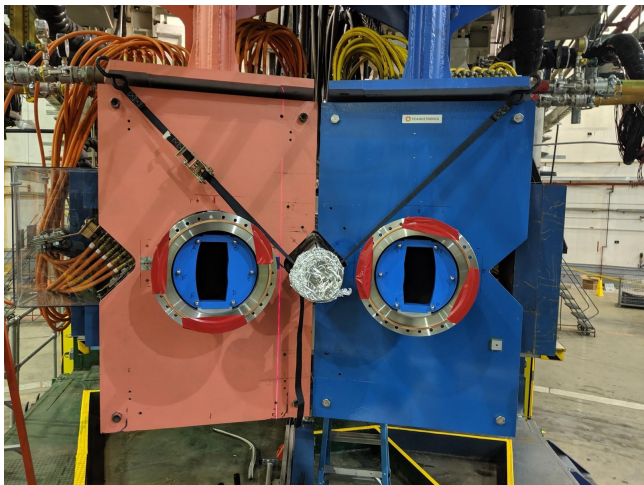


- Started with**
- Single puck
 - 5 mm thick
 - 96% ^{48}Ca , 3.84% ^{40}Ca

- Ended with**
- 1 puck + 2 foiles sandwiched
 - ~ 5.7 mm thick
 - 91.7% ^{48}Ca , 7.96% ^{40}Ca



	Energy (GeV)	Θ (Degrees)	Q^2 (GeV^2)
^{48}Ca	2.18	4.51	0.0297



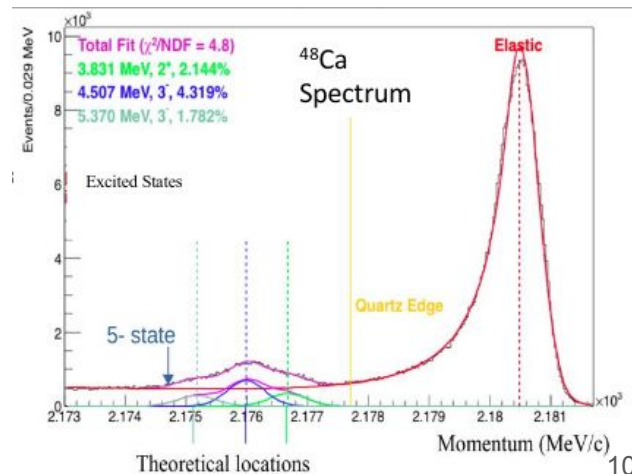
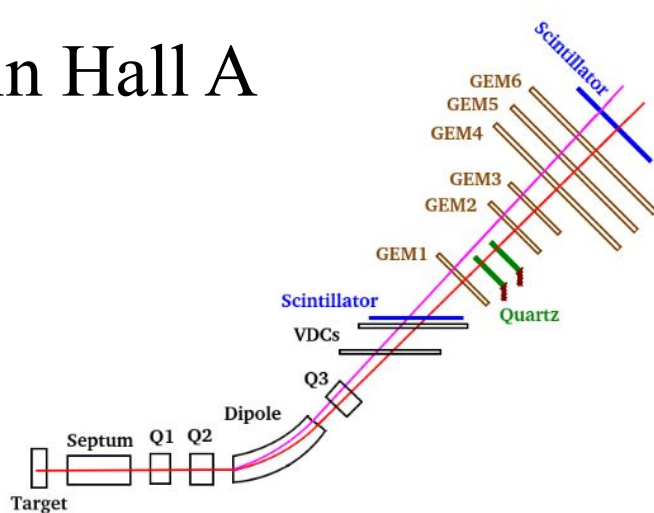
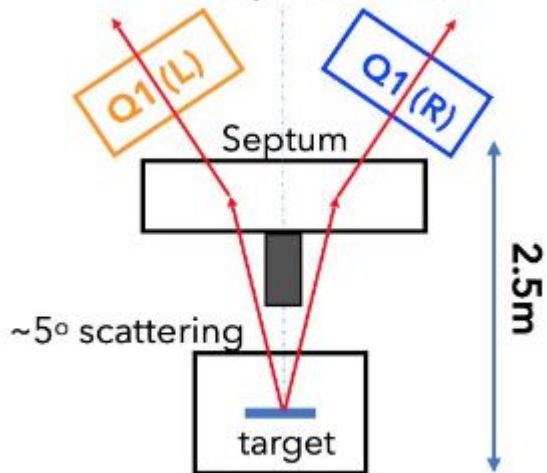
~12.5^o spectrometers

Measuring A_{pV} in Hall A

Q1 collimators to define acceptance

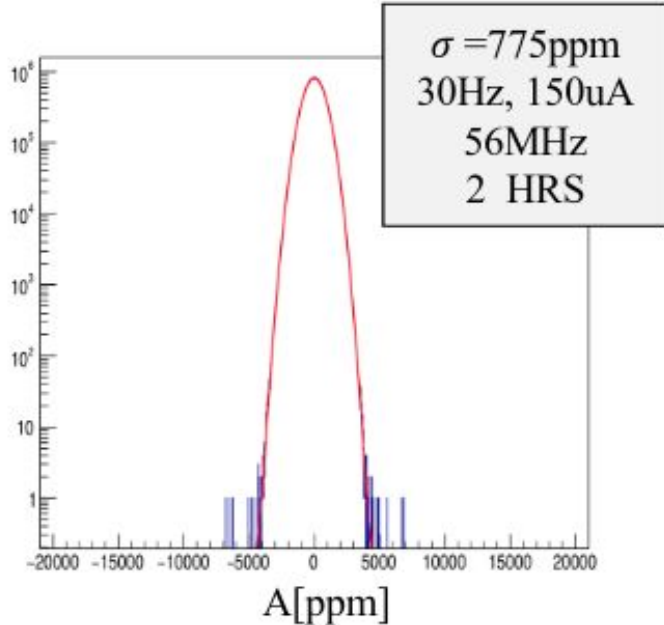
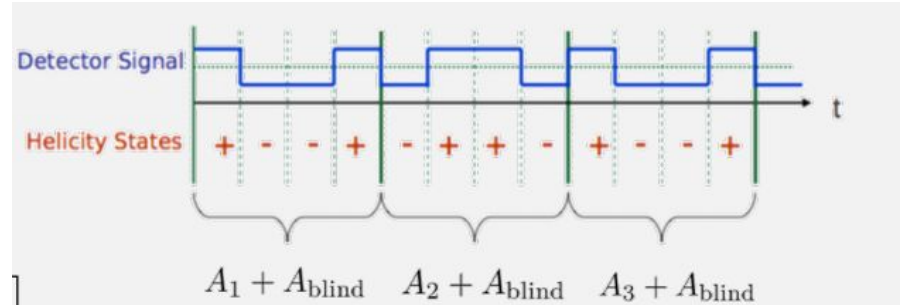
HRS (QQDQ) tuned to separate inelastically scattered electrons from the elastic ones. Elastically scattered electrons focused onto main detectors

Septum to bend electrons into HRS aperture



Measuring A_{PV} in Hall A

$$A_{PV} = \frac{\sigma_R - \sigma_L}{\sigma_R + \sigma_L}$$



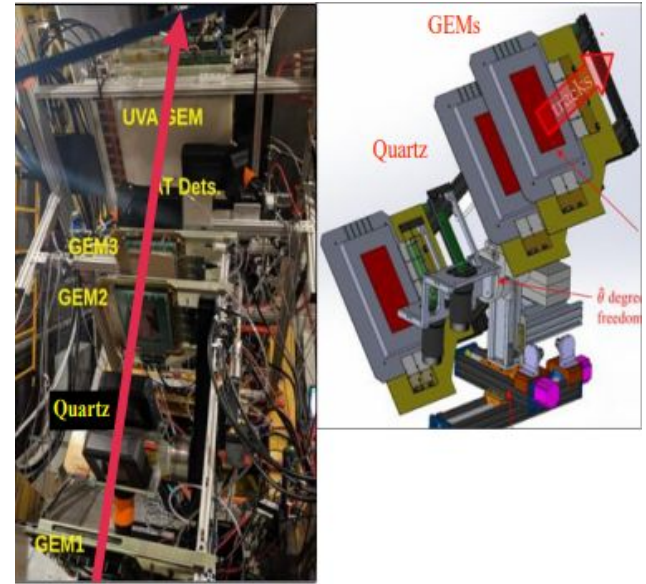
- Integrating measurement, not counting
- 30 Hz helicity window, 120 Hz flip rate
- Production running totalled 412 C $\sim 2.6 \times 10^{21}$ electrons
- ~ 300 million flips or ~ 80 million quartets
- Measurement dominated by counting statistics

Integrating Detectors



- 5 mm thick quartz Cherenkov detector with $16 \times 3.5 \text{ cm}^2$ area coupled to a PMT
- 56 MHz integrating rate in both arms
- Linearity measurements done pre/post running and during the run

Counting Detectors



- Flexible design to do counting ($<1 \text{ uA}$) measurements
- VDCs below detector stand, with GEMs installed upstream and downstream detectors
- Used for alignment of elastic peak onto detectors and kinematics measurements

Extracting the Physics Asymmetry

Asymmetry extraction requires a lot of work with careful analysis of systematics

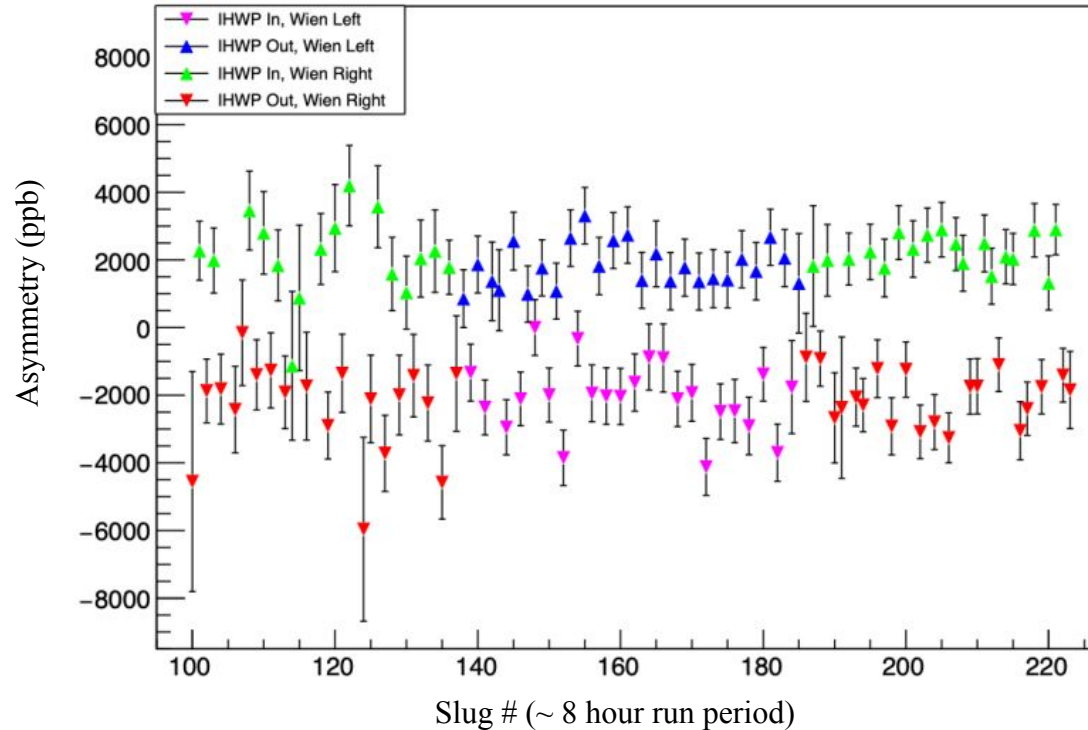
$$A_{phys} = R_{radcorr} R_{accept} R_{Q^2} \frac{A_{corr} - P_L \sum_i f_i A_i}{P_L (1 - \sum_i f_i)}$$

$$A_{corr} = A_{det} - A_{beam} - A_{trans} - A_{nonlin} - A_{blind}$$

- A_{beam} (beam corrections)
- A_{trans} (**transverse asymmetry**)
- A_{nonlin} (detector nonlinearity)
- A_{blind} (blinding factor)
- $P_L \sum_i f_i A_i$ (**backgrounds**)
- $1 - \sum_i f_i$ (**background dilution**)
- P_L (**longitudinal polarization**)
- R_{Q^2} (Q^2 scaling)
- R_{accept} (**acceptance**)
- R_{radcor} (radiation)

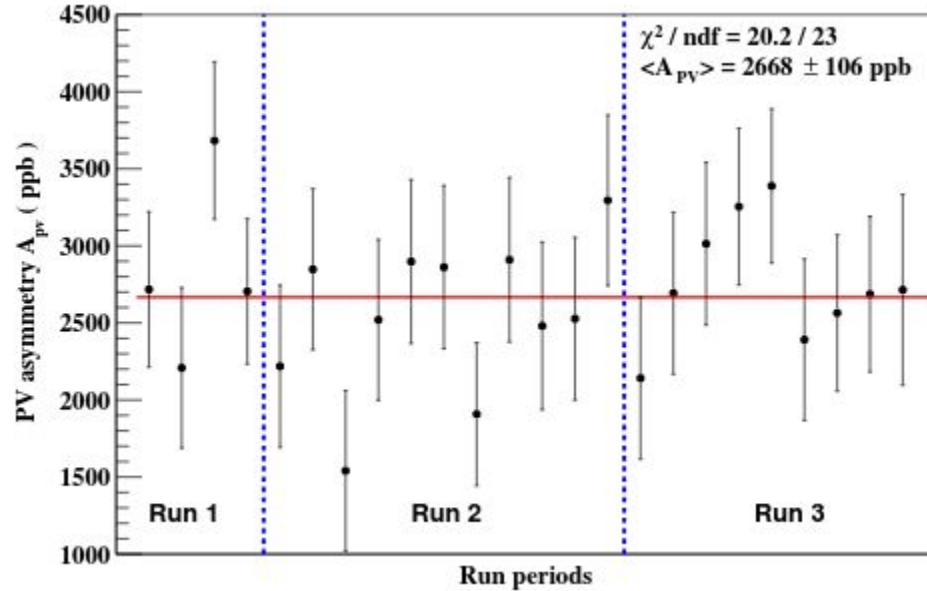
Largest relative contributions to the systematics. Largest background from 1st E.S of ^{48}Ca

^{48}Ca Asymmetry Measurements



$$A_{\text{PV}} = 2668 \pm 106 \text{ ppb (4.0\%)} \pm 40 \text{ ppb (1.5\%)}$$

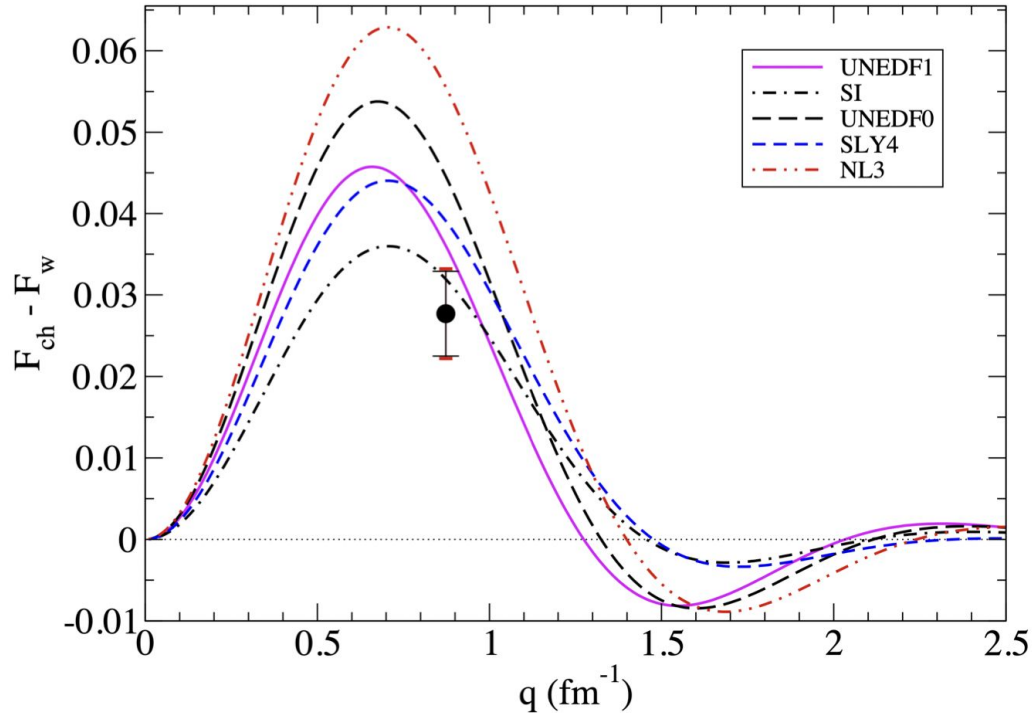
^{48}Ca Asymmetry Measurements



~ 40 hour run periods

Three run periods separated by different injector spin configurations - Run 3 taken post COVID shutdown

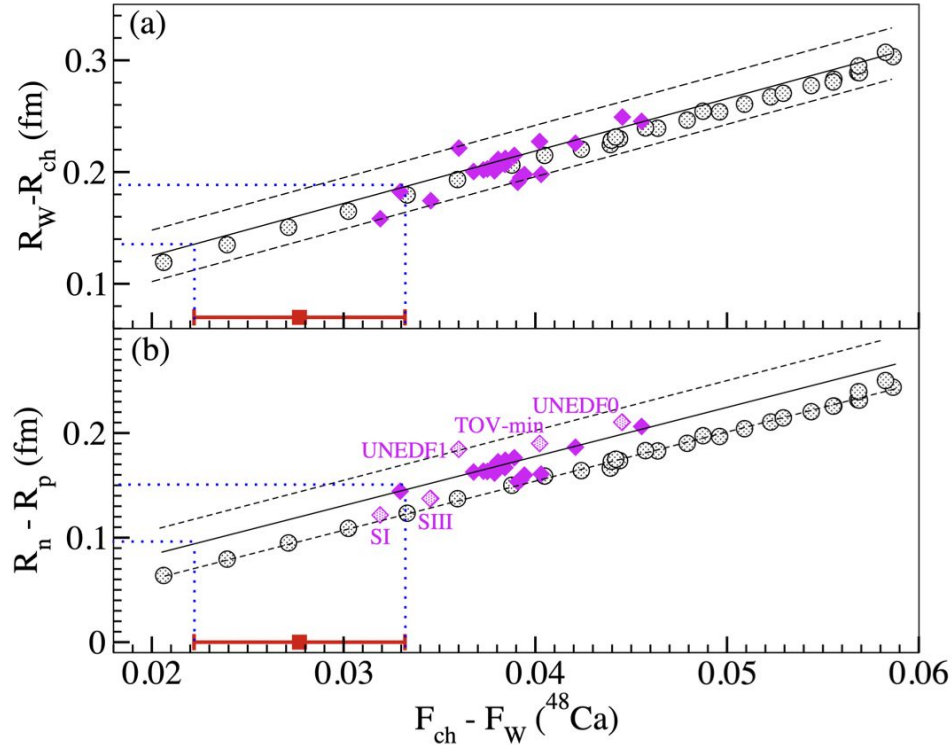
From A_{pV} to Neutron Skin



Red - total experimental error, black - stat error

- Directly translate A_{pV} to F_w and $F_{ch} - F_w$ using Coulomb corrections and empirical $F_{Ch}(Q^2)$
- $F_{ch} - F_w$ is the primary result which is model-independent
- Different DFT models show different q dependence
- CREX q introduces slight model dependence in the extraction of R_w and $R_w - R_{ch}$

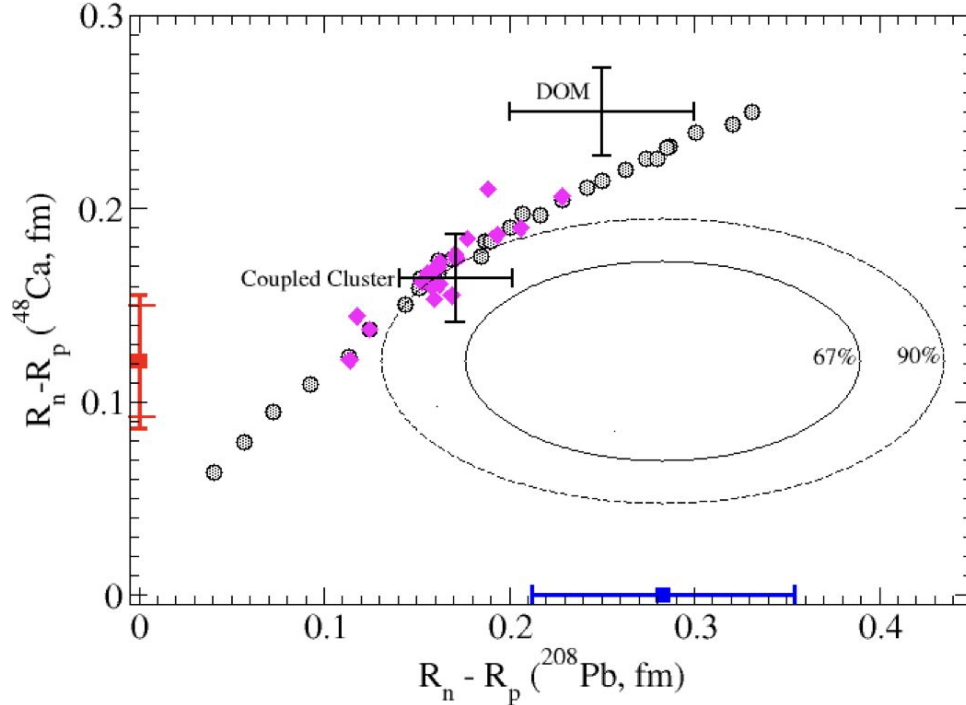
From A_{pV} to Neutron Skin



- From F_w introduce small nuclear model dependence (surface thickness or fall off)
- From $F_{ch} - F_w$ to neutron skin must include nuclear effects such as spin-orbit corrections

Quantity	Value \pm (exp) \pm (model) [fm]
$R_W - R_{ch}$	$0.159 \pm 0.026 \pm 0.023$
$R_n - R_p$	$0.121 \pm 0.026 \pm 0.024$

Comparing CREX/PREX Neutron Skin to Theory



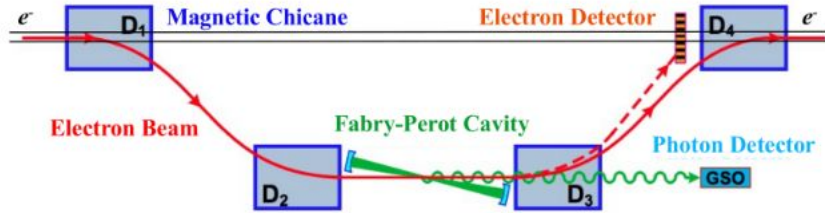
- CREX data is consistent with the microscopic coupled cluster models slightly over predicting ^{48}Ca , while slightly under predicting ^{208}Pb
- Dispersive optical models agree well with ^{208}Pb but substantially over predict ^{48}Ca

Summary

- New precise measurement for the parity-violating asymmetry of ^{48}Ca
- Model-independent extraction of the weak form factor
- Weak skin and neutron skin extracted with small model dependence
- CREX result implies thinner skin compared to models, while PREX implies a thicker skin compared to models
- CREX result is consistent with a variety of density functional theories and microscopic coupled cluster calculations

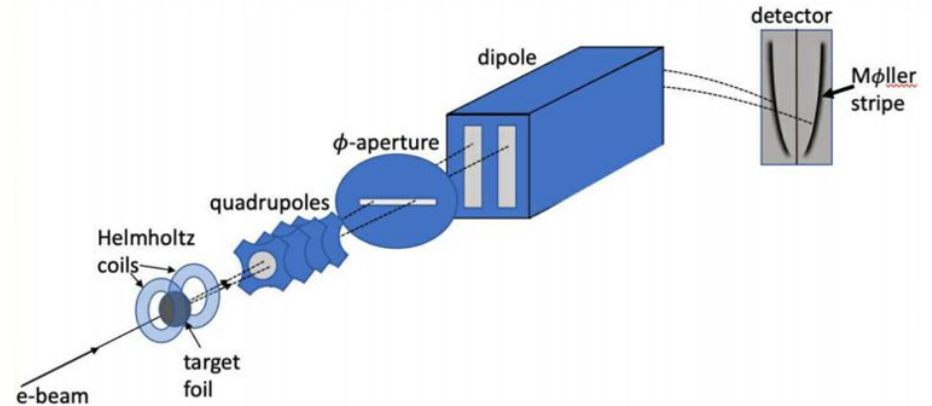
Backups

Polarimetry



Compton Polarimeter

- Continuous non-invasive measurement
- 4 dipole configuration
- Electrons scatter of CP light in FP
- Backscattered photons measured by GSO
- Scattered from unscattered separated by 3rd dipole. Scattered measured by electron detector while unscattered bent by 4th dipole on target



Moller Polarimeter

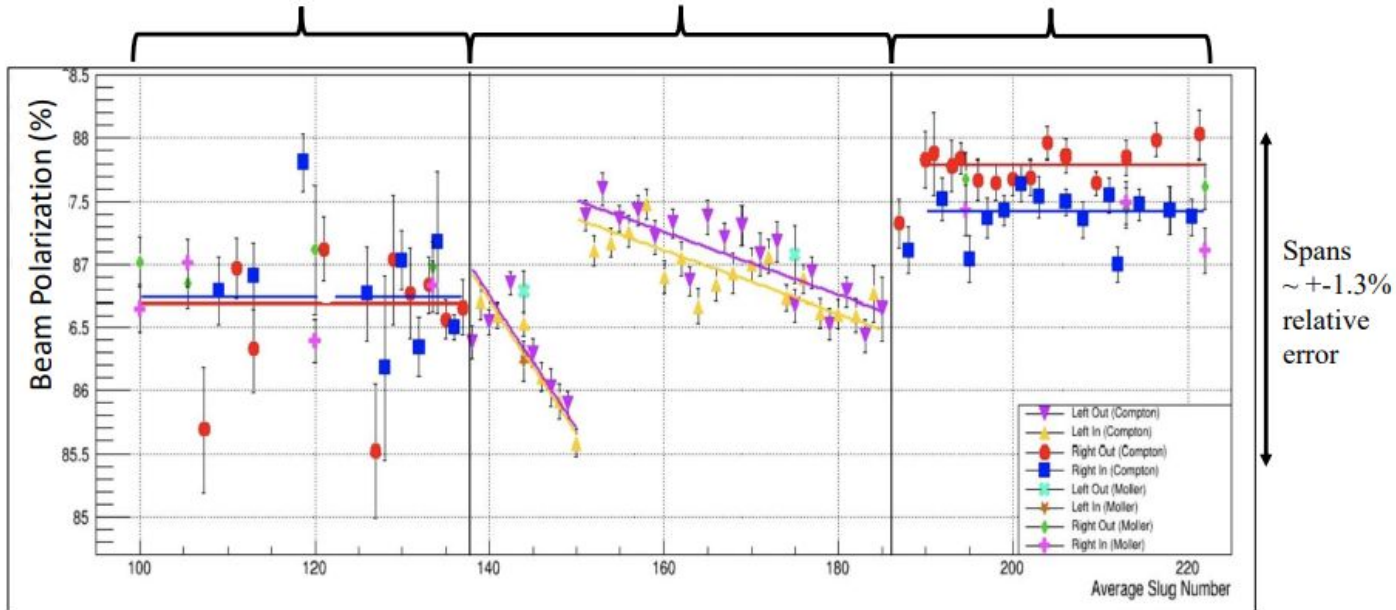
- Low current invasive measurement - Once a week
- Beam scatter off magnetized Fe foil using 3-4 T solenoidal field

Compton and Moller Results

1st period Spring 2020
Right (In/Out)

2nd period Spring 2020
Left (In/Out)

3rd period Summer 2020
Right (In/Out)



Acknowledgments: A.J. Zec, J. C. Cornejo, M. Dalton, C. Gal, D. Gaskell, C. Palatchi, K. Paschke, A. Premithilake, B. Quinn

Compton

$$P_e = 87.10 \pm (0.52\% \text{ dP/P})$$

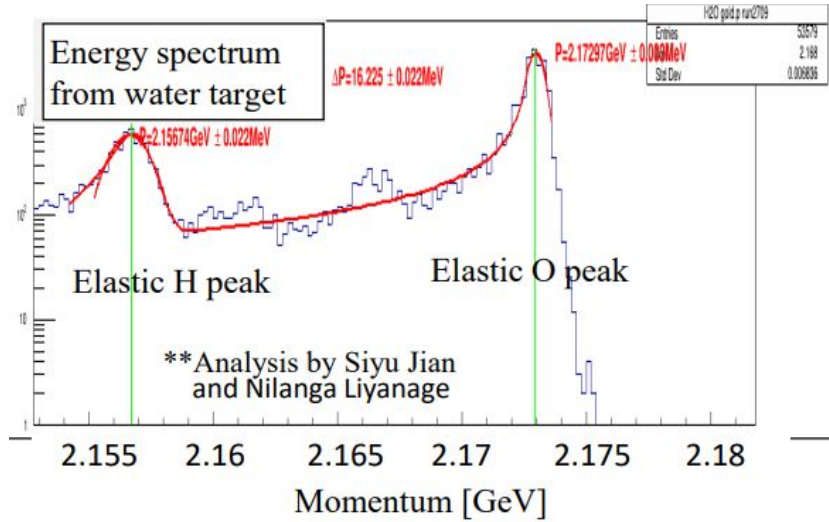
CREX Polarimetry Result

$$P_e = 87.09 \pm (0.44\% \text{ dP/P})$$

Moller

$$P_e = 87.06 \pm (0.85\% \text{ dP/P})$$

Scattering Angle Calibration



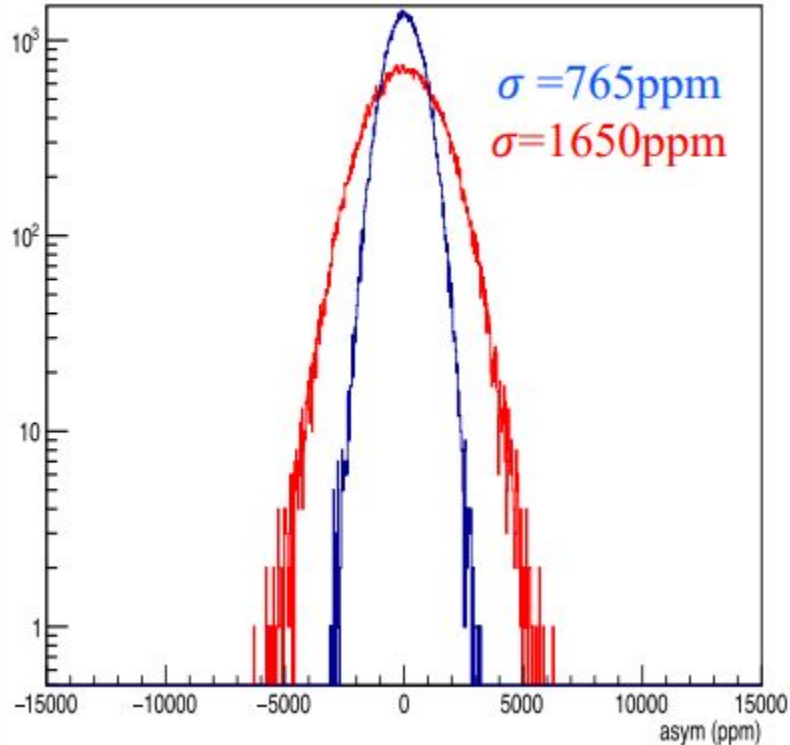
- Nuclear Recoil
- ^1H and ^{16}O in same target with same energy loss provides a measurement of the scattering angle
- Central angle measurement with precision of $\delta\theta = 0.02^\circ$ (0.45%)

Recoil Momentum Difference -> Scattering Angle

$$\Delta E' = E'_O - E'_H = E \left(\frac{1}{1 + \frac{2E \sin^2(\frac{\theta}{2})}{M_O}} - \frac{1}{1 + \frac{2E \sin^2(\frac{\theta}{2})}{M_H}} \right)$$

Beam Corrections

Ap, Raw (red) vs. Corrected (blue)



- Beam jitter larger than counting statistics
- Analysis techniques used to remove beam jitter

$$A_{\text{corr}} = A_{\text{raw}} - \alpha \Delta E + \sum_i \square_i \Delta x_i$$

- Measured since helicity correlated beam asymmetries are systematic errors
- Measure full phase space of beam jitter (energy, position, angle)
- Multiple techniques to calibrate detector response (α , \square_i)

Beam Corrections Techniques

$$A_{\text{corr}} = A_{\text{raw}} - \alpha \Delta E + \sum_i \beta_i \Delta x_i$$

Regression

$$\chi^2 = \sum (A_{\text{raw}} - \sum_i \beta_i \Delta M_i)^2, \quad \frac{\partial \chi^2}{\partial \beta_i} = 0$$

Dithering

$$\frac{\partial \hat{D}}{\partial C_\mu} = \sum_{i=1}^{N_{BPM}} \beta_i \frac{\partial M_i}{\partial C_\mu}, \quad \beta_i = \frac{\partial \hat{D}}{\partial M_i},$$

for $\mu = 1, 2, \dots, N_{\text{coil}}$, and can be solved if

$$N_{\text{coil}} \geq N_{BPM}.$$

Lagrange -- a combination of the above two

$$\mathcal{L} = \chi^2 + \sum_\mu \lambda_\mu \left(\frac{\partial D}{\partial C_\mu} - \sum_i \beta_i \frac{\partial M_i}{\partial C_\mu} \right),$$

χ^2 minimization with beam modulation sensitivities constraints:

$$\frac{\partial \mathcal{L}}{\partial \beta_i} = 0, \quad \frac{\partial \mathcal{L}}{\partial \lambda_\mu} = 0$$

Regression: Detector Response measured using natural beam fluctuations (χ^2 minimization)

Dithering: Modulate beam parameters above the full phase space of the jitter ○

Lagrange: Combination of the two

Systematics

Correction	Absolute [ppb]	Relative [%]
Beam polarization	382 ± 13	14.3 ± 0.5
Beam trajectory & energy	68 ± 7	2.5 ± 0.3
Beam charge asymmetry	112 ± 1	4.2 ± 0.0
Isotopic purity	19 ± 3	0.7 ± 0.1
3.831 MeV (2^+) inelastic	-35 ± 19	-1.3 ± 0.7
4.507 MeV (3^-) inelastic	0 ± 10	0 ± 0.4
5.370 MeV (3^-) inelastic	-2 ± 4	-0.1 ± 0.1
Transverse asymmetry	0 ± 13	0 ± 0.5
Detector non-linearity	0 ± 7	0 ± 0.3
Acceptance	0 ± 24	0 ± 0.9
Radiative corrections (Q_W)	0 ± 10	0 ± 0.4
Total systematic uncertainty	40 ppb	1.5%
Statistical uncertainty	106 ppb	4.0%

Weak Interaction sees Neutrons

	Proton	Neutron
Electric Charge	1	0
Weak Charge	0.08	1

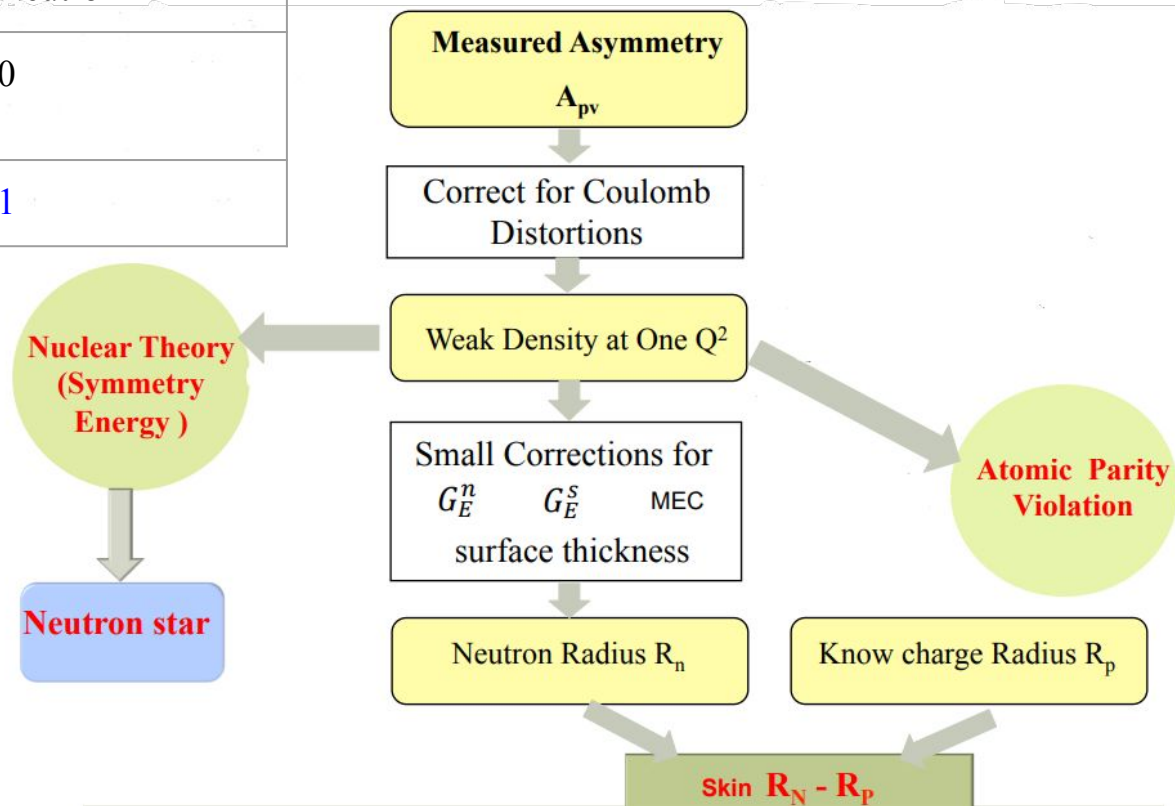


Figure from Y. Tian